

This item is the archived peer-reviewed author-version of:

Nanoscale analysis of historical paintings by means of O-PTIR spectroscopy : the identification of the organic particles in L'Arlésienne (portrait of Madame Ginoux) by Van Gogh

Reference:

Beltran Victoria, Marchetti Andrea, Nuyts Gert, Leeuwestein Margje, Sandt Christophe, Borondics Ferenc, De Wael Karolien.- Nanoscale analysis of historical paintings by means of O-PTIR spectroscopy : the identification of the organic particles in L'Arlésienne (portrait of Madame Ginoux) by Van Gogh
Angewandte Chemie: international edition in English - ISSN 1521-3773 - 60:42(2021), p. 22753-22760
Full text (Publisher's DOI): <https://doi.org/10.1002/ANIE.202106058>
To cite this reference: <https://hdl.handle.net/10067/1799890151162165141>

Nanoscale analysis of historical paintings by means of O-PTIR spectroscopy: The identification of the organic particles in *L'Arlésienne (portrait of Madame Ginoux)* by Van Gogh

Victoria Beltran^{+[a,b]}, Andrea Marchetti^{+[a,b]}, Gert Nuyts^[a,b], Margje Leeuwestein^[c], Christophe Sandt^[d], Ferenc Borondics^[d], Karolien De Wael* ^[a,b]

- [a] Dr. V. Beltran, Dr. A. Marchetti, Mr. G. Nuyts, Prof. K. De Wael
AXES research group, University of Antwerp
Groenenborgerlaan 171, 2020, Antwerp, Belgium
E-mail: karolien.dewael@uantwerpen.be
- [b] Dr. V. Beltran, Dr. A. Marchetti, Mr. G. Nuyts, Prof. K. De Wael
NanoLab Center of Excellence, University of Antwerp
Groenenborgerlaan 171, 2020, Antwerp, Belgium
- [c] Mrs. M. Leeuwestein
Kröller-Müller Museum
Houtkampweg 6, 6731 AW Otterlo, Netherlands
- [d] Dr. C. Sandt, Dr. F. Borondics
Synchrotron SOLEIL
F-91192 Gif-sur-Yvette, France

[+] These authors contributed equally to this work.

Supporting information for this article is given via a link at the end of the document

Abstract: Optical-photothermal infrared (O-PTIR) spectroscopy is a recently developed technique that provides spectra comparable to traditional transmission FTIR spectroscopy with nanometric spatial resolution. Hence, O-PTIR is a promising candidate for the analysis of historical paintings, as well as other cultural heritage objects, but its potential has not yet been evaluated.

This work presents the first application of O-PTIR to the analysis of cultural heritage, and in particular to an extremely small fragment from Van Gogh's painting *L'Arlésienne (portrait of Madame Ginoux)*. The striking results obtained, including the detection of geranium lake pigments as well as the complete analysis of the stratigraphy, failed with other state-of-the-art techniques, highlight the potential of this method. The integration of O-PTIR to the study of cultural heritage opens to the possibility of decreasing the amount of sample extracted, therefore contributing to the preservation of the integrity of artworks while providing a complete characterization of the materials.

Introduction

The composition of historical paintings tends to be highly heterogeneous. In addition to the main compounds, there are often materials present in a very low proportion which can be either intrinsic to the artworks^[1–4] or related to the ageing of the object and its past conservation treatments^[5,6].

One type of minor components detected in samples from historical paintings are the micrometric particles and layers, sometimes <10 μm diameter/thickness. Such features can be related to the physical properties of the object (such as the color of specific regions)^[7–9] or to specific degradation processes (such as the migration or aggregation of molecules)^[10,11]. The characterization of these compounds is therefore a fundamental requirement in order to understand the composition, physical properties and historical background of the object and/or to decipher possible degradation reactions. Obtaining this information is the first step to find the appropriate preventive

measures and/or conservation treatments to avoid or minimize further deterioration, hence it is of capital importance.

Unfortunately, the identification of these micrometric areas can be extremely complex due to the limited amount of sample available for the analysis, which must be minimized if possible in order to ensure the preservation of the artworks integrity. Moreover, the samples often contain a wide diversity of materials, including ionic compounds, organic and inorganic materials with low and high molecular weight: the higher proportions of these materials and their related signals hide the weak features from the minor compounds making their detection difficult.

Previous studies have shown the potential of high spatial resolution techniques such as X-ray based methods to characterize inorganic particles and layers^[12,13]. Nonetheless, there are still open questions regarding the most suitable method for the discrimination of the organic ones. For this purpose, former research applied micro Fourier Transform Infrared (μFTIR) spectroscopy and μRaman spectroscopy, that provide information on the molecular structure as well as the spatial distribution of the compounds. However, the spatial resolution of μFTIR spectroscopy is low: the minimum size achievable is restricted by the diffraction limit to 3–15 μm depending on the wavelength, consequently the bands of the spectral markers of the areas <10 $\mu\text{m} \times 10 \mu\text{m}$ are often too low to be unequivocally detected.^[14] On the other hand, Raman spectroscopy can reach a higher spatial resolution ($\geq 1 \mu\text{m}$ diameter for the 785nm laser), but it is often limited by the presence of fluorescence and the potential damage that might be caused on sensitive materials^[15–17]. Lately, photothermal induced resonance (PTIR) has been applied to the analysis of paintings^[10,18]: this technique uses an atomic force microscope (AFM) coupled to infrared spectroscopy providing a spatial resolution up to 20 nm (size of the cantilever), which has been proved to successfully characterize organic materials in painting samples^[10,19]. However, this technique requires a continuous contact between the cantilever and the sample surface. In the case of painting fragments, normally very brittle, this requirement is problematic due to 1) the small particles often detached from the surface during the handling of the samples, these crumbles remain on the surface disturbing the path of the cantilever which produce interferences in the collected data and

RESEARCH ARTICLE

II) the brittleness of the materials makes it difficult to have a totally flat surface, these imperfections (detached particles, cracks or protrusions) alter the path of the cantilever and may lead to the damage of the thin section or the cantilever tip.

In this work, we investigate for the first time the potential of optical-photothermal infrared (O-PTIR) spectroscopy applied to the analysis of organic particles from historical paintings. O-PTIR is a recently developed device based on the thermal expansion of the sample induced by the irradiation with an IR laser, which is then measured using a visible probe laser. Thus, the spatial resolution of O-PTIR is determined by the spot size of the visible laser, overcoming the diffraction limit that defines the resolution achievable by FTIR spectroscopy (Figure S1). Besides its high spatial resolution, typically well below 1 μm , O-PTIR measurements do not require contact with the sample, avoiding the interferences with the detached particles or potential damages to the analyzed fragment. Moreover, the collected spectra are comparable to transmission FTIR measurements^[20–22], allowing the comparison between the collected data and the extensive literature on FTIR spectroscopy applied to cultural heritage materials^[23–25]. Thanks to these features, O-PTIR is a promising technique for the analysis of historical paintings, as well as other cultural heritage objects with polychromed surfaces, however its potential has not yet been evaluated.

In this study, this technique was applied, in particular, to the characterization of the stratigraphy and the identification of the pink pigment particles ($\leq 2 \mu\text{m}$ diameter) observed in the paint layer of the Vincent van Gogh's painting *L'Arlésienne (portrait of Madame Ginoux)* (February 1890, oil on canvas, Kröller-Müller Museum) (Figure 1). The striking results obtained demonstrate the potential of O-PTIR for the molecular characterization of small painting fragments and the identification of micrometric features. In fact, with the suitable sample preparation, O-PTIR provided high spatial resolution data while preserving the sample's integrity. Based on these results, it is therefore demonstrated that O-PTIR is a powerful technique that can be efficiently integrated in multitechnique studies, thus helping to complement and extend the information provided with other analytical methods.

Results and Discussion

3.1. Potential of O-PTIR for the characterization of thin layers from historical paintings

The sample selected for these experiments comes from the historical painting *L'Arlésienne (portrait of Madame Ginoux)* from Van Gogh. Due to the high artistic and historical value of this painting, the extracted fragment is very small, $\approx 200 \mu\text{m} \times 200 \mu\text{m} \times 25 \mu\text{m}$ (Figure 1, top). As it can be seen in the thin section (Figure 1, bottom), the stratigraphy consists of a bottom layer made of canvas fibers ($\approx 10\text{--}20 \mu\text{m}$ thickness), a thin white ground layer ($\approx 10 \mu\text{m}$ thickness) and finally a thin top paint layer with pink particles ($\approx 10 \mu\text{m}$ thickness). The presence of such thin layers, poses great challenges for the characterization of the stratigraphy. In order to verify the potential of O-PTIR for the analysis of paint fragments, it is essential to compare it with existing methods already established. In this case, the samples were analyzed by μFTIR spectroscopy coupled to Synchrotron Radiation ($\mu\text{SR-FTIR}$ spectroscopy): this technique provides a high spatial resolution with a high signal-to-noise ratio and, for these reasons, it is widely employed for the molecular characterization of thin paint layers.^[26,27] The $\mu\text{SR-FTIR}$ spectroscopy measurements were performed in transmission mode, which provides the best spectral resolution while minimizing spectral artifacts such as baseline drifts due to scattering. The obtained results were compared to O-PTIR, in order to verify the opportunities and the possible constraints of this technique. The same thin section was analyzed with both methods, in order to ensure the comparability of the datasets (Figure 2).

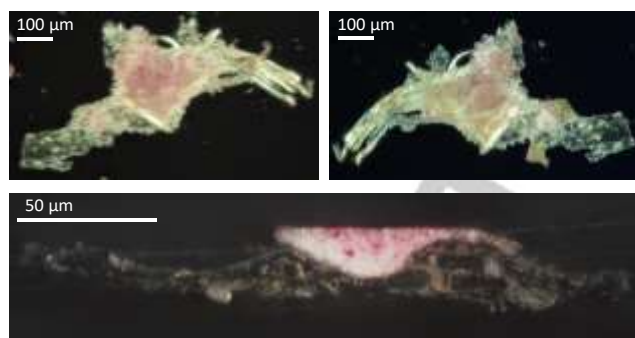


Figure 1. Fragment of the painting *L'Arlésienne (portrait of Madame Ginoux)* from Van Gogh selected for the analysis. Top: fragment before embedding (front and back). Bottom: thin section of the embedded fragment.

The results obtained by $\mu\text{SR-FTIR}$ spectroscopy are displayed in Figure 2 (top). Overall, the spectra are characterized by a high spectral quality (high signal to noise ratio and flat baseline) typical of $\mu\text{SR-FTIR}$. Among the collected data, five main types of spectra can be distinguished (Figure 2, top right corner, the full range of the spectra is displayed in Figure S2). The main pigment identified is lead white ($2\text{PbCO}_3 \cdot \text{Pb}(\text{OH})_2 / \text{PbCO}_3$), whose markers can be seen at ≈ 1390 and 1045 cm^{-1} (asymmetric and symmetric C-O stretching vibrations of CO_3^{2-} anions respectively^[28]). Additionally, the spectra of lead white also show smaller amounts of CaCO_3 , which is detected by the shoulder at 1453 and the small band at 874 cm^{-1} (C-O stretching and bending of the CO_3^{2-} anions respectively^[29]). The band at $\approx 1734 \text{ cm}^{-1}$ is probably associated to the presence of a drying oil, which was most likely used as a binder. In some regions, this band shows a shoulder at $\approx 1709 \text{ cm}^{-1}$ corresponding to the hydrolysis of the esters from the drying oil, which is a degradation reaction linked to its ageing^[30]. The presence of Pb and Ca was confirmed by SEM-EDX, agreeing with the identification of lead white and CaCO_3 (Figure 3). These painting materials were previously identified in other paintings by the same artist^[31–34].

In addition, the results also indicate the presence of protein (bands at ≈ 1660 and 1543 cm^{-1} , related to amide I and amide II respectively^[35]) and cellulose (bands at 1114 , 1062 and 1037 cm^{-1} , related to the C-O bending of the skeletal vibration of carbohydrates rings, HCHOH deformation and the skeletal vibration of the carbohydrate rings^[36]). These compounds correspond to the support of the painting, in this case a canvas coated with a sizing^[37]: the cellulose is related to the textile fibers and the protein to the animal glue used as an adhesive. Finally, the spectra of the epoxy resin used to embed the sample can also be discriminated. It should be mentioned that the most intense bands (1512 cm^{-1} related to the C=C stretching of the aromatic groups and at 1247 cm^{-1} related to the C-O deformation^[38]) are also noticeable in the other displayed $\mu\text{SR-FTIR}$ spectra: this is probably explained by the spot size of this technique, which is too big to select only regions inside of the sample. Consequently, the analyzed areas usually include regions outside the paint fragment, where there is only embedding medium, or regions close to the edge of the sample, where the embedding medium has been infiltrated. Hence, the bands of epoxy resin are also present in the spectra.

Compared to $\mu\text{SR-FTIR}$, the spectra collected by O-PTIR (Figure 2, bottom right corner) display similar spectral features, allowing to discriminate most of the compounds previously mentioned. Moreover, thanks to its higher spatial resolution, it is possible to discriminate the spectra of lead white and drying oil from the spectra of CaCO_3 and drying oil, demonstrating that these pigments have a different spatial distribution. No band shifts are observed between both techniques and the relative intensities of the bands are globally similar: this can be clearly seen in the

RESEARCH ARTICLE

spectra of epoxy resin, which is the only homogeneous compound (the fluctuations in the other spectra may be explained by the different composition of the precise analyzed spot). Furthermore, O-PTIR spectra do not show the bands related to the embedding medium, contrarily to μ SR-FTIR. Since the analyzed thin section is the same in both techniques, this difference is probably explained by the size of the analyzed area in each technique. The smaller spot size of O-PTIR compared to μ SR-FTIR allows to select areas far away from the edge of the sample, providing spectra free of epoxy bands. The lack of the epoxy bands in the spectra helps to avoid their overlapping with the signal from other compounds, preventing the loss of spectral features and potentially allowing a more efficient discrimination of the different components of the sample. For instance, a broad

shoulder centered at $\approx 1550\text{ cm}^{-1}$ is noticeable in the O-PTIR spectra, probably related to the presence of metal carboxylates^[11]. In the μ SR-FTIR data, on the contrary, this shoulder is overlapped with the band at $\approx 1510\text{ cm}^{-1}$ from epoxy resin, therefore the presence of metal carboxylates is less obvious. Consequently, the O-PTIR data is extremely useful for the analysis of micrometric/submicrometric features from heterogeneous samples, often the case for painting cross sections. The spectral markers of the identified compounds were integrated in order to obtain the spatial distribution of each substance by each technique (Figure 2, top and bottom left corners), the look-up tables (LUT) of the maps and the position of the displayed spectra in the integration maps is shown in Figure S3.

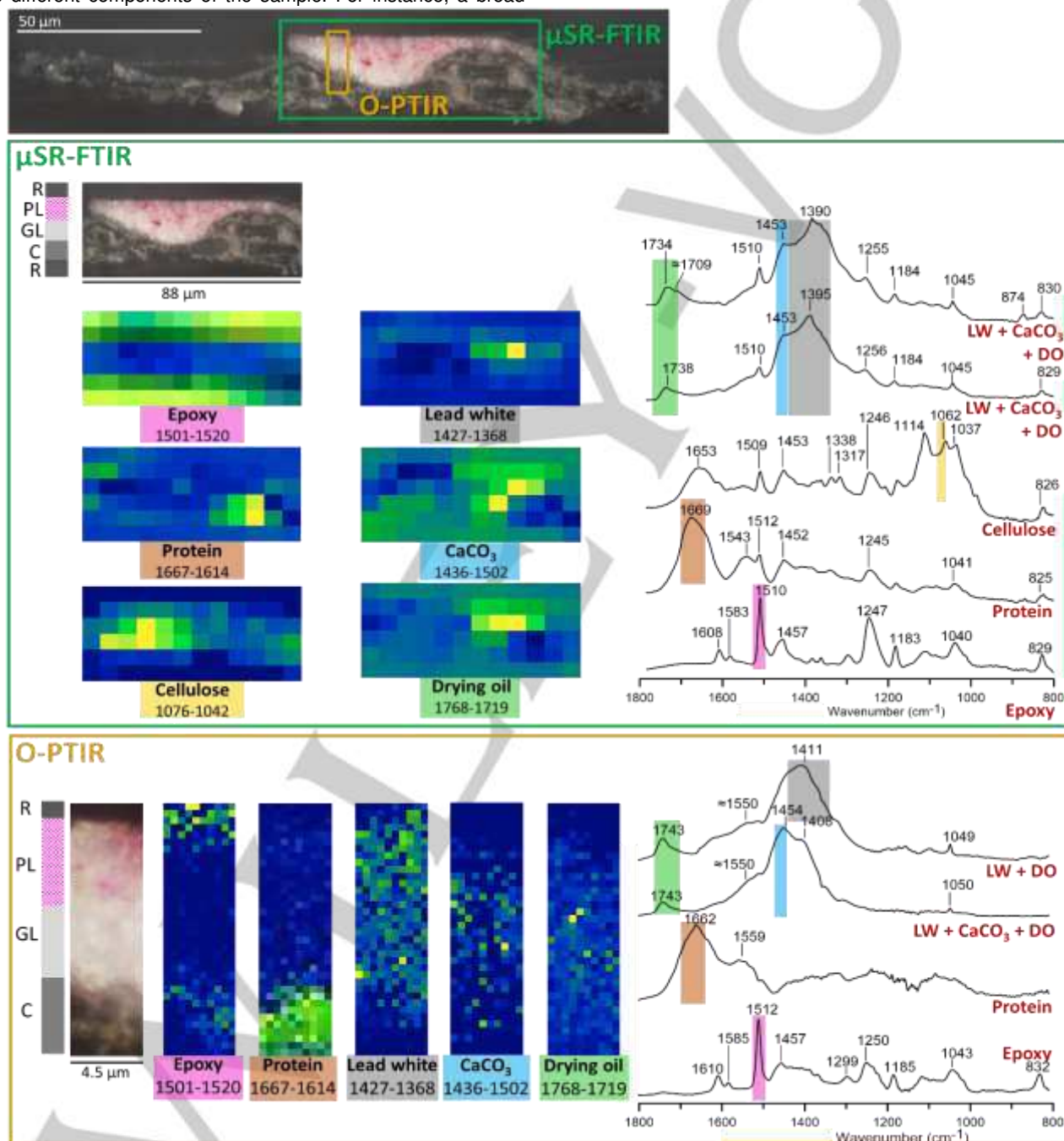


Figure 2. Analysis by μ SR-FTIR and O-PTIR of the thin section displayed in Figure 1. Top: μ SR-FTIR results of the area marked in green (spot size: $10\text{ }\mu\text{m} \times 10\text{ }\mu\text{m}$). Bottom: O-PTIR results of the area marked in yellow (spot size: $450\text{ nm} \times 450\text{ nm}$). In each analyzed area a scheme of the stratigraphy is displayed (C: canvas, GL: ground layer, PL: paint layer, R: embedding resin) as well as the integration maps of the spectral regions corresponding to the specific compounds found in the sample and a representative spectrum of each material (LW: lead white, DO: drying oil).

RESEARCH ARTICLE

Due to the lower spatial resolution, μ SR-FTIR maps are much less detailed, providing only the main distribution of the compounds: epoxy resin around the sample, protein and cellulose at the bottom of the stratigraphy and CaCO_3 , lead white and drying oil in the ground and paint layers. On the contrary, the maps calculated from O-PTIR spectra allowed to distinguish also the variations of the composition across the thin layers of the stratigraphy: the ground layer is composed mainly of drying oil and lead white, while the paint layer contains drying oil, lead white and CaCO_3 . Specifically, CaCO_3 is distributed mainly in the middle of the stratigraphy. This distribution is in good agreement with the results obtained by SEM-EDX (Figure 3).

A consequence of the high spatial resolution of O-PTIR is the length of the measurements. Since the number of acquired spectra is larger, the required time for the analysis is much longer. In this case, the area analyzed by μ SR-FTIR spectroscopy is $88 \mu\text{m} \times 40 \mu\text{m}$ (Figure 2, top) and took ≈ 3 hours, while the area analyzed by O-PTIR is $4.5 \mu\text{m} \times 17.5 \mu\text{m}$ (Figure 2, bottom) and took ≈ 10 hours. The slower data collection implies that the maps should be smaller and, hence, less representative. In this case, for instance, cellulose was not detected by O-PTIR because it is present outside of the analyzed area. In addition, it should be remarked that the signal-to-noise ratio is slightly lower in O-PTIR compared to μ SR-FTIR. In the higher range of the O-PTIR spectra the noise level is still low, although subtle features such as the shoulder at $\approx 1710 \text{ cm}^{-1}$ related to the degradation of the drying oil cannot be appreciated. However, the noise is more evident at lower wavenumbers: for instance, the band at 874 cm^{-1} related to CaCO_3 cannot be distinguished in O-PTIR.

Considering the limits and possibilities of this technique, the high spatial resolution of O-PTIR can provide a precise characterization of the micro- and nanoheterogeneities which, integrated in a multianalytical approach, provides an accurate characterization of the samples. Additionally, it should be mentioned that the size of the produced data is not significantly higher: the acquired O-PTIR map is around 4 Mb while the μ SR-FTIR map is around 9 Mb.

In conclusion, these results confirm the suitability of O-PTIR for the high spatial resolution analysis of the stratigraphy of historical paintings. The obtained spectra are comparable to the ones obtained by μ SR-FTIR allowing to identify the same type of compounds. Despite the lower signal-to-noise ratio of O-PTIR compared to μ SR-FTIR, the smaller spot size provides more site specific spectra and hence less overlapped, helping to better

discriminate the compounds present in the sample. This higher spatial resolution offers accurate information on the distribution of materials, helping to better characterize the materials and techniques used to produce the painting as well as its conservation state. It is clear that such information can have great relevance for the study and conservation of historical paintings.

Moreover, the results also demonstrated the great advantages of the preparation of thin sections for the analysis by O-PTIR. This technique can be applied to non-embedded fragments however, the preparation of thin sections allows the compatibility of the obtained dataset with other complementary techniques, such as transmission μ SR-FTIR spectroscopy and SEM-EDX, but also Raman spectroscopy or μ SR-XRD^[38,39]. This is extremely relevant, since it means that these techniques are fully compatible and can be implemented in the same multi-analytical approach.

3.2. Application of O-PTIR for the identification of micrometric heterogeneities: discrimination of the pink pigment

In the paint layer of the sample, small pink particles of $\leq 2 \mu\text{m}$ diameter can also be observed (Figure 1). Their characterization is extremely relevant, since it can provide information on the composition of the pink color of the sampled area of the painting. However, the analysis of these particles is challenging due to their low proportion, their small size and the presence of additional compounds in the same layer.

Indeed, the analysis by μ SR-FTIR spectroscopy (Figure 2) did not provide any spectral marker that may be related to this pigment, most probably due to the low spatial resolution of the technique. The size of the particles is in fact very small compared to the size of the analyzed spot, so the spectral markers are hidden below the spectra of the main compounds, whose bands cover broad spectral regions. Consequently, there are no noticeable bands that could be attributed to the material used as a pigment.

In order to improve the spatial resolution, μ Raman spectroscopy using a 785 nm laser was also tested (Figure 4). The spectra collected around one of the pink particles show the characteristic bands from lead white at 1048 and 104 cm^{-1} as well as a group of bands around $\approx 200 \text{ cm}^{-1}$ probably related to the degradation products resulting from this pigment.^[40] Moreover, a group of low-intensity bands can be seen at ≈ 1430 , ≈ 1307 and $\approx 1249 \text{ cm}^{-1}$

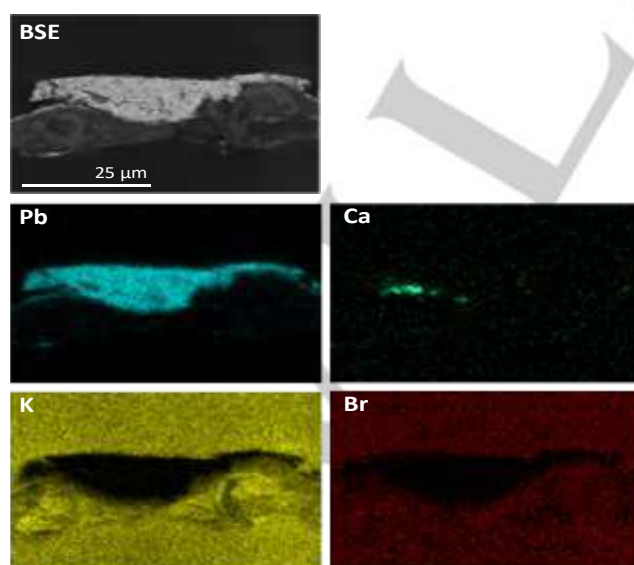


Figure 3. Analysis of the thin section displayed in Figure 1 by SEM-EDX. Left: image obtained from BSE. Right: elemental distribution maps. The elements in the second row (K, Br) are related to the KBr pellet used as a substrate.

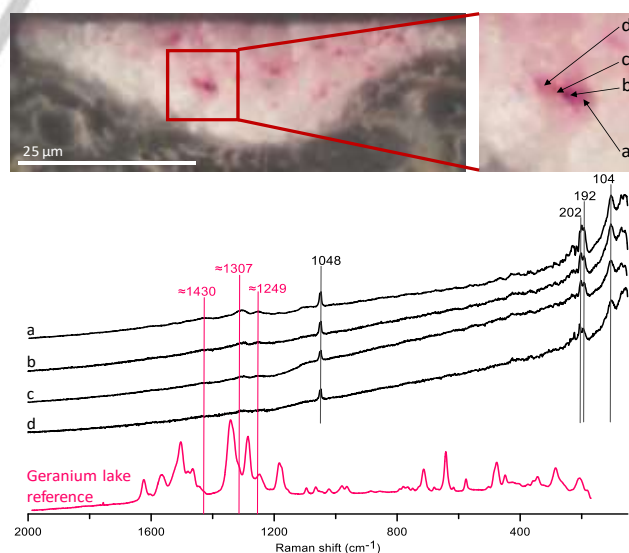


Figure 4. Characterization of a pink particle by μ Raman spectroscopy. Top: analyzed particle (left) and its magnification where the points analyzed have been marked, a-d (right). Bottom: Raman spectra collected compared to a reference of geranium lake (pink line) (synthesis conditions described in SI, section 1.2). The peaks marked in pink are presumably associated to geranium lake pigments, the bands marked in black correspond to lead white and the degradation products resulting from this pigment.

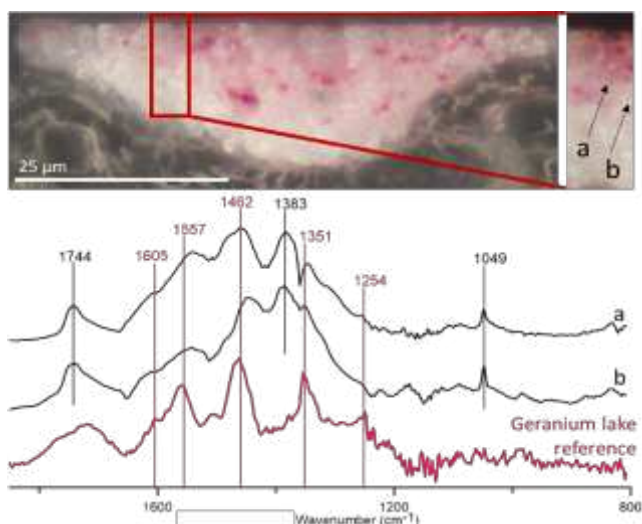


Figure 5. Characterization of the pink particles by O-PTIR spectroscopy. Top: region selected for the analysis (left) and its magnification with the analyzed points in evidence, a-b (right). Bottom: O-PTIR spectra collected at each point and reference spectrum of freshly synthesized geranium lake obtained by the same technique (synthesis conditions described in SI, section 1.2). The peaks marked in pink correspond to geranium lakes.

(Figure 4, bands marked in pink). These bands are in the spectral region where some of the main bands of the pink pigments from the family of geranium lakes appear, as it can be seen in the reference spectrum (Figure 4, spectra in pink), meaning that the presence of these pigments is compatible with the results. However, the bands are low, broad and the maximums are slightly shifted from the ones described in literature^[41]. Moreover, these signals appear in the same region of other lake pigments employed by the same artist, such as cochineal^[34,42,43]. Therefore, the identification of the type of pigment cannot be unambiguously concluded based in these results.

Interestingly, the application of O-PTIR made it possible to overcome the limitations previously encountered with both μ SR-FTIR and μ Raman spectroscopies. This novel technique, in fact, allowed to unequivocally identify the particles in exam as a geranium lake pigment (Figure 5). The collected spectra (Figure 5, spectra in black) clearly show the main bands of geranium lakes observed in the reference of the pigment analyzed by the same technique (Figure 5, spectrum in red). In particular, the bands at ≈ 1550 and ≈ 1460 (carboxylate group), ≈ 1605 , ≈ 1351 and ≈ 1254 (xanthene and ketone groups) of geranium lakes can be identified^[41]. It should be remarked that the spectra include also the bands from the other compounds previously detected in the sample: among them lead white and lead carboxylates show bands at ≈ 1450 and ≈ 1550 cm^{-1} that overlap with the peaks of geranium lakes producing slight shifts in the bands. Nonetheless the low intensity of the band at 1045 cm^{-1} related to lead white and the lack of an intense band at 1400 cm^{-1} where lead carboxylates normally have a main signal suggest that the intensity of the peaks related to both substances is low enough to confidently detect geranium lakes.

It should be also mentioned that the minimum at 1359 cm^{-1} is probably an instrumental artifact linked to the chip transitions of the laser (Figure S4). However, this does not affect the presence of a clear shoulder at 1351 cm^{-1} linked to the composition of the sample. The fact that this shoulder and also the shoulder at 1605 cm^{-1} cannot be assigned to any other compound previously detected in the sample, and that the obtained spectra are clearly different from the IR spectrum of cochineal lakes^[44,45] as well as from madder lakes^[46,47] also used by Van Gogh, unequivocally confirms the presence of geranium lakes in the painting in exam. Due to the overlap with the bands from other compounds it is not

possible to map the distribution of geranium lakes in the sample. Nonetheless, the selected spectra are located in the pink paint layer, clearly highlighting the link between the presence of geranium lakes and the color of the paint film.

Geranium lakes have been previously observed in other paintings by Van Gogh^[33,34,43,48,49]. The use of this family of pigments is normally deduced from the detection of Br in pink colored areas, however the identification of the pigment molecules is difficult since they are normally mixed with drying oil containing similar functional groups, namely carboxyls, carbonyls and C=C bonds. In the case of the painting in analysis, the detection is even more challenging due to the co-presence in the same paint layer of lead white, lead carboxylates and CaCO_3 , whose intense bands at ≈ 1400 , ≈ 1550 and ≈ 1450 cm^{-1} respectively overlap with geranium lakes. Hence, the molecular detection of geranium lakes proves the great potential of O-PTIR for the analysis of micro- and nano-heterogeneities, even in adverse conditions.

In order to corroborate the identification of geranium lakes, the presence of Br in the pigment particles was analyzed by SEM-EDX (Figure 6). The analyses were performed using a low energy (10 KeV) in order to decrease the penetration in the sample and thus avoid the interference from the KBr pellet used as a substrate. Due to the low amount of pigment it was not possible to map the presence of Br. Nonetheless, it is noticeable that the spectrum collected in the paint layer where the pink color is observed shows the presence of small amounts of Br (Figure 6c), while this element cannot be found in the ground layer (Figure 6, b) or in the embedding medium (Figure 6, a). Therefore, the presence of Br is correlated to the pigment particles in exam, which is in agreement with the use of geranium lakes in the painting.

Since geranium lake pigments are well known to degrade in the presence of visible light^[34,50], it is important to verify if the visible laser used by O-PTIR could cause any damage to the sample, potentially hampering further analysis by other techniques. This eventuality was tested by collecting a series of replicate O-PTIR analyses on the same spot of a reference sample (Figure 7), which have then compared to a previous spectrum of this material obtained by conventional FTIR spectroscopy. The results show that the spectrum collected by FTIR spectroscopy is very similar to the ones obtained by OPTIR, both the initial (Figure 7, t_0) and the final obtained after 22 repetitions (18 minutes) (Figure 7, t_1), hence proving that O-PTIR, with the suitable experimental parameters, has not caused a noticeable damage to this sensitive material. For this reason, the technique can be considered as non-destructive in terms of sample for the type of materials considered in this study.

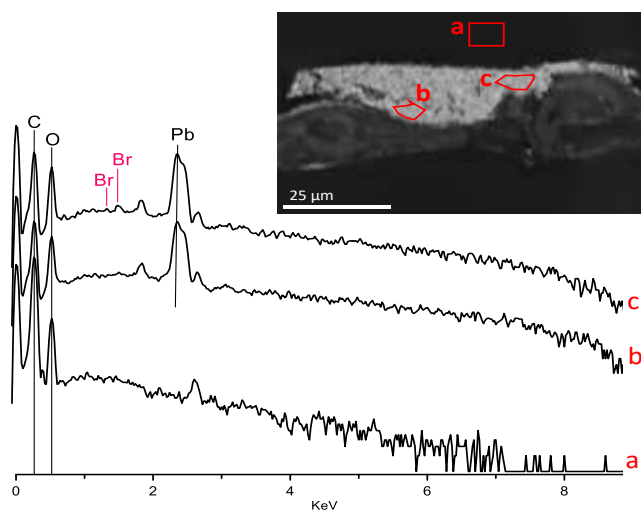


Figure 6. Characterization of the paint layer by SEM-EDX. BSE image (top), the regions marked in red correspond to the areas where the EDX spectra (bottom) were collected: a) embedding medium, b) ground layer and c) paint layer.

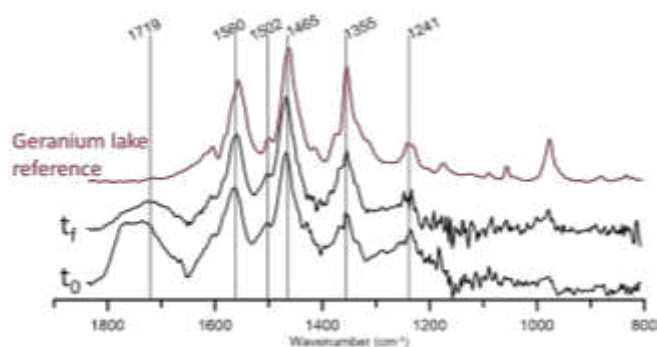


Figure 7. Study of the potential radiation damage on a reference sample of geranium lake (synthesis conditions described in SI, section 1.2) during O-PTIR analysis. Previous FTIR spectrum (pink) compared to OPTIR: initial spectrum (t_0) and spectrum after irradiate the sample during 22 consecutive accumulations (t).

Conclusion

In this study, the application of O-PTIR spectroscopy to the analysis of samples from historical paintings is presented for the first time. This technique allowed to identify the pink particles present in a small fragment from the historical painting *L'Arlésienne (portrait of Madame Ginoux)* by Van Gogh as geranium lake pigments, while preserving the sample's integrity. Due to the limited size of these particles and the presence of additional compounds, the other analytical techniques tested, namely μ SR-FTIR and μ Raman spectroscopy, were not able to unambiguously identify this material.

The high spatial resolution offered by O-PTIR, which pushes the boundaries of traditional molecular spectroscopy by overcoming the diffraction limits of traditional FTIR, presents great advantages for the analysis of paintings and heritage objects in general. This allows, in fact, an accurate chemical characterization of the stratigraphy, even when only micrometric fragments are available. Thanks to this high spatial resolution, O-PTIR does not only provide less overlapped spectra, helping to identify micro- and nano-heterogeneities in the samples, but also allows to decrease the size of the samples needed for the analysis. This presents clear advantages for the study and preservation of cultural heritage, maximizing the obtainable information while minimizing the invasive sampling of the objects, hence contributing to the preservation of the integrity of artworks.

Moreover, although thin samples are not inherently necessary for O-PTIR, the technique appeared highly efficient for the analysis of thin sections of embedded painting fragments. The suitability of this sample preparation for O-PTIR analysis highlights the compatibility of this technique with other commonly employed characterization methods, hence opening to the possibility of a full integration of O-PTIR in multitechnique studies of cultural heritage objects.

Acknowledgements

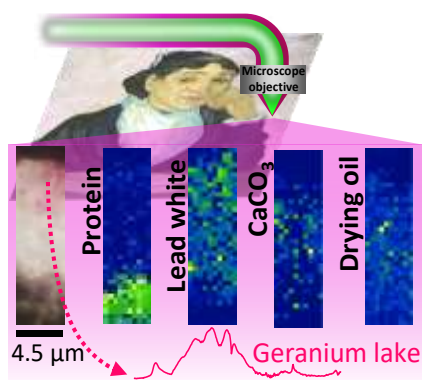
The authors acknowledge the financial support of Brain-be Belspo (funded project: ARTGARDEN Art Technical Research and Preservation of Historical Mixed-Media Ensembles: 'Enclosed Gardens'), of the BOF-SEP (funded project: Diagnostics for Artworks) and of FWO agency under the call "FWO Medium Size Research Infrastructure" (funded project: High resolution Raman spectroscopy and imaging). Moreover, the authors acknowledge the funding received to perform the μ SR-FTIR and O-PTIR experiments in Synchrotron Soleil (beamtime proposal 20191722).

Keywords: vibrational spectroscopy • IR spectroscopy • O-PTIR • historical paintings • Van Gogh

- [1] A. Cesaratto, M. Leona, J. R. Lombardi, D. Comelli, A. Nevin, P. Londero, *Angew. Chemie* **2014**, *126*, 14601–14605.
- [2] A. Serrano, A. van den Doel, M. van Bommel, J. Hallett, I. Joosten, K. J. Van den Berg, *Anal. Chim. Acta* **2015**, *897*, 116–127.
- [3] N. Salvadó, S. Butí, M. A. G. Aranda, T. Pradell, *Anal. Methods* **2014**, *6*, 3610.
- [4] H. de la Codre, M. Radepon, J. Echard, O. Belhadj, S. Vaiedelich, V. Rouchon, *X-Ray Spectrom.* **2020**, xrs.3160.
- [5] V. Gonzalez, A. Van Loon, S. Wt Price, P. Noble, K. Keune, *J. Anal. At. Spectrom.* **2020**, *35*, 2267–2273.
- [6] H. Tan, H. Tian, J. Verbeeck, L. Monico, K. Janssens, G. Van Tendeloo, *Angew. Chemie Int. Ed.* **2013**, *52*, 11360–11363.
- [7] F. S. Welsh, *J. Am. Inst. Conserv.* **1988**, *27*, 55.
- [8] H. Tan, H. Tian, J. Verbeeck, L. Monico, K. Janssens, G. Van Tendeloo, *Angew. Chemie Int. Ed.* **2013**, *52*, 11360–11363.
- [9] N. Salvadó, S. Butí, M. A. G. Aranda, T. Pradell, *Anal. Methods* **2014**, *6*, 3610–3621.
- [10] X. Ma, V. Beltran, G. Ramer, G. Pavlidis, D. Y. Parkinson, M. Thoury, T. Meldrum, A. Centrone, B. H. Berrie, *Angew. Chemie Int. Ed.* **2019**,
- [11] F. Casadio, K. Keune, E. Hendriks, S. A. Centeno, Eds., *Metal Soaps in Art. Conservation and Research*, Springer International Publishing, **2019**.
- [12] M. Alfeld, L. de Viguerie, *Spectrochim. Acta - Part B At. Spectrosc.* **2017**, *136*, 81–105.
- [13] M. Cotte, A. Genty-Vincent, K. Janssens, J. Susini, *Comptes Rendus Phys.* **2018**, *19*, 575–588.
- [14] R. Salzer, H. W. Siesler, *Infrared and Raman Spectroscopic Imaging*, Wiley-VCH, Weinheim, **2014**.
- [15] G. D. Smith, L. Burgio, S. Firth, R. J. H. Clark, *Anal. Chim. Acta* **2001**, *440*, 185–188.
- [16] A. De Santis, E. Mattei, C. Pelosi, *J. Raman Spectrosc.* **2007**, *38*, 1368–1378.
- [17] D. L. A. De Faria, S. Venâncio Silva, M. T. De Oliveira, *J. Raman Spectrosc.* **1997**, *28*, 873–878.
- [18] S. Morsch, B. A. Van Driel, K. J. Van Den Berg, J. Dik, *ACS Appl. Mater. Interfaces* **2017**, *9*, 10169–10179.
- [19] S. Morsch, B. A. Van Driel, K. J. Van Den Berg, J. Dik, *ACS Appl. Mater. Interfaces* **2017**, *9*, 10169–10179.
- [20] J. A. Refner, *Spectroscopy* **2018**, *33*, 12–17.
- [21] N. Baden, H. Kobayashi, N. Urayama, *Int. J. Polym. Anal. Charact.* **2020**, *25*, 1–7.
- [22] O. Klementieva, C. Sandt, I. Martinsson, M. Kansiz, G. K. Gouras, F. Borondics, *Adv. Sci.* **2020**, *7*, 1903004.
- [23] M. Derrick, D. Stulik, J. Landry, *Infrared Spectroscopy in Conservation Science*, **2000**.
- [24] C. Daher, C. Paris, A.-S. Le Hô, L. Bellot-Gurlet, J.-P. Échard, *J. Raman Spectrosc.* **2010**, *41*, 1494–1499.
- [25] E. Casanova, C. Pelé-Meziani, É. Guilminot, J. Y. Mevellec, C. Riquier-Bouclet, A. Vinçotte, G. Lemoine, *Anal. Methods* **2016**, *8*, 8514–8527.
- [26] N. Salvadó, S. Butí, M. J. Tobin, E. Pantos, A. J. N. W. Prag, T. Pradell, *Anal. Chem.* **2005**, *77*, 3444–3451.
- [27] M. Cotte, P. Dumas, Y. Taniguchi, E. Checroun, P. Walter, J. Susini, *Comptes Rendus Phys.* **2009**, *10*, 590–600.

- [28] O. Siidra, D. Nekrasova, W. Depmeier, N. Chukanov, A. Zaitsev, R. Turner, *Acta Crystallogr. Sect. B Struct. Sci. Cryst. Eng. Mater.* **2018**, *74*, 182–195.
- [29] H. Böke, S. Akkurt, S. Özdemir, E. H. Göktürk, E. N. Caner Saltik, *Mater. Lett.* **2004**, *58*, 723–726.
- [30] L. De Viguerie, P. A. Payard, E. Portero, P. Walter, M. Cotte, *Prog. Org. Coatings* **2016**, *93*, 46–60.
- [31] M. Geldof, A. N. Proaño Gaibor, F. Ligterink, E. Hendriks, E. Kirchner, *Herit. Sci.* **2018**, *6*, 1–20.
- [32] E. Kirchner, I. van der Lans, F. Ligterink, M. Geldof, A. Ness Proano Gaibor, E. Hendriks, K. Janssens, J. Delaney, *Color Res. Appl.* **2018**, *43*, 158–176.
- [33] J. E. Fieberg, P. Knutás, K. Hostettler, G. D. Smith, *Appl. Spectrosc.* **2017**, *71*, 794–808.
- [34] A. Distel, S. A. Stein, *Cézanne to Van Gogh: The Collection of Doctor Gachet*, Metropolitan Museum Of Art, **1999**.
- [35] B. S. Krimm, J. Bandekart, *Adv. Protein Chem.* **1986**, *38*, 181–364.
- [36] O. Faix, J. Bremer, O. Schmidt, S. J. Tatjana, *J. Anal. Appl. Pyrolysis* **1991**, *21*, 147–162.
- [37] S. Hackney, *On Canvas: Preserving the Structure of Paintings*, Getty Publications, Los Angeles, **2020**.
- [38] V. Beltran, N. Salvadó, S. Butí, G. Cinque, K. Wehbe, T. Pradell, *Anal. Chem.* **2015**, *87*, 6500–6504.
- [39] N. Salvadó, S. Butí, V. Beltran, T. Pradell, C. Clemente, J. Juanhuix, G. Cinque, *Pure Appl. Chem.* **2017**, *90*.
- [40] L. Burgio, R. J. H. Clark, S. Firth, *Analyst* **2001**, *126*, 222–227.
- [41] V. Beltran, A. Marchetti, S. De Meyer, G. Nuyts, K. De Wael, *Dye. Pigment.* **2021**, *189*, 109260.
- [42] F. Pozzi, J. R. Lombardi, M. Leona, *Herit. Sci.* **2013**, *1*, 23.
- [43] S. A. Centeno, C. Hale, F. Carò, A. Cesaratto, N. Shibayama, J. Delaney, K. Dooley, G. van der Snickt, K. Janssens, S. A. Stein, *Herit. Sci.* **2017**, *5*, 1–11.
- [44] K. Haberová, V. Jančovičová, D. Veselá, Z. Machatová, M. Oravec, *Dye. Pigment.* **2021**, *186*, 108971.
- [45] J. Kirby, M. Spring, C. Higgitt, *Natl. Gall. Tech. Bull.* **2007**, *28*, 69–95.
- [46] C. Clementi, B. Doherty, P. L. Gentili, C. Miliani, A. Romani, B. G. Brunetti, A. Sgamellotti, *Appl. Phys. A Mater. Sci. Process.* **2008**, *92*, 25–33.
- [47] G. Zhuang, S. Pedetti, Y. Bourlier, P. Jonnard, C. Méthivier, P. Walter, C. M. Pradier, M. Jaber, *J. Phys. Chem. C* **2020**, *124*, 12370–12380.
- [48] K. A. Dooley, A. Chieli, A. Romani, S. Legrand, C. Miliani, K. Janssens, J. K. Delaney, *Angew. Chemie* **2020**, *132*, 6102–6109.
- [49] M. Vellekoop, L. Jansen, M. Geldof, E. Hendriks, A. de Tagle, Eds., *Van Gogh's Studio Practice*, Yale University Press, New Haven, **2013**.
- [50] A. Chieli, C. Miliani, I. Degano, F. Sabatini, P. Tognotti, A. Romani, *Dye. Pigment.* **2020**, *181*, 108600.

Entry for the Table of Contents



The application of Optical-photothermal infrared (O-PTIR) spectroscopy to the analysis of the organic composition of samples from historical paintings is presented for the first time. Thanks to its high resolution, thin layers ($\approx 10\text{-}20\ \mu\text{m}$ thickness) and small particles ($\leq 2\ \mu\text{m}$ diameter) have been successfully characterized.

Institute Twitter usernames: axesgroup, synchroSOLEIL, krollermuller